# Modeling a self-propelled autochemotactic walker

Johannes Taktikos,[1] Vasily Zaburdaev,[1,2] and Holger Stark[1]
[1]*Institut für Theoretische Physik, Technische Universität Berlin, Hardenbergstraße 36, D-10623 Berlin, Germany*
[2]*School of Engineering and Applied Science, Harvard University, 29 Oxford Street, Cambridge, Massachusetts 02138, USA*
(Received 27 July 2011; published 21 October 2011)

We develop a minimal model for the stochastic dynamics of microorganisms where individuals communicate via autochemotaxis. This means that microorganisms, such as bacteria, amoebae, or cells, follow the gradient of a chemical that they produce themselves to attract or repel each other. A microorganism is represented as a self-propelled particle or walker with constant speed while its velocity direction diffuses on the unit circle. We study the autochemotactic response of a single self-propelled walker whose dynamics is non-Markovian. We show that its long-time dynamics is always diffusive by deriving analytic expressions for its diffusion coefficient in the weak- and strong-coupling case. We confirm our findings by numerical simulations.

DOI: 10.1103/PhysRevE.84.041924 PACS number(s): 87.17.Jj, 05.10.Gg, 45.50.−j

## I. INTRODUCTION

The motion of biological organisms ranging from the microscopic world of bacteria to larger cells up to social insects represents an interesting area of current research where the interdisciplinary link between biology and statistical physics manifests itself. In this article we propose a model for microorganisms whose motion is governed by chemotactic signaling [1]. Unlike a diffusion process that is characterized by unbiased movement, chemotaxis results in a directed flow of particles ("taxis") to spatial regions of higher or lower concentration of a chemical [2–4]. The first case is called positive chemotaxis due to a chemoattractant and the latter negative chemotaxis due to a chemorepellent. To be more precise, chemotaxis denotes the ability of a microorganism to orient its velocity direction along the chemical's gradient [4]. Chemotaxis is ubiquitous in systems of bacteria and eukaryotic cells: Wound healing in the human body is enabled by the directed motion of granulocytes to the region of injury, chemotaxis makes sperm cells find their way to the ovum, and almost all kinds of animals can smell and detect food sources [4]. If the chemical is produced by the microorganisms themselves, the system exhibits "autochemotaxis," which serves as a possible mechanism for communication between them. Two preeminent and well-studied examples showing autochemotaxis are the social amoeba *Dictyostelium discoideum* as well as the intestinal bacterium *Escherichia coli* [5,6].

An additional motivation to study chemotaxis is to describe the clustering of bacteria into microcolonies, which contributes to the early stage of biofilm formation [7,8]. There is a huge scientific concern to understand biofilm characteristics, for instance, in bacteriology, where the knowledge of bacterial survival strategies seems essential to prevent the formation of biofilms in clinical devices [9].

The first quantitative chemotaxis model by Keller and Segel takes a continuum approach and has been variously generalized [10–13]. One of the classical derivations of the Keller-Segel model applies the framework of continuous-time random walks [14]. A derivation of this type requires assumptions for statistical properties on a microscopic level, such as run length or velocity turning distributions. In contrast, we explicitly describe the Langevin dynamics of individual microorganisms. In our approach, the microorganisms are considered as entities with constant speed, independent of the chemical's gradient or concentration itself. This fact constitutes a major difference to the models in Refs. [15,16] where the particles are not active *per se* as only the presence of a concentration gradient induces a nonzero mean speed. In our model, the particle speed represents an additional parameter and chemotaxis only influences the velocity direction.

Due to the complexity of a nonequilibrium system consisting of self-propelled microorganisms, one can only address a few averaged macroscopic quantities of interest. Accordingly, calculating the long-time diffusion coefficient of interacting or self-propelled particles has been the key purpose of numerous publications; see, for instance, Refs. [15–23].

The main goal of this article is to investigate the influence of autochemotaxis on a particle's long-time diffusion coefficient. To obtain analytical results, we restrict ourselves to the study of a single particle. In contrast to several approaches using perturbation theory [15,18], our results also hold for strong chemotactic interactions. In the case of positive autochemotaxis, it is clear that the particle will be attracted to recently explored regions where it has emitted chemoattractant. As a consequence the particle's motion will be restricted in comparison to a freely diffusing nonchemotactic microorganism. So the question arises whether the particle will eventually be trapped, in the sense that the long-time diffusion coefficient vanishes, as is the case in a two-dimensional model by Tsori and de Gennes [24], or whether the motion becomes diffusive in the long-time limit where the mean-squared displacement grows linearly in time [16,19,25]. Note that recent experimental results also inspired the study of chemotaxis models with anomalous subdiffusion and superdiffusion [26]. We will show that in our model even for strong chemotactic coupling the particle motion will be diffusive. We will derive analytical expressions that approximate its long-time diffusion coefficient.

This article is organized as follows. In Sec. II A we introduce in detail our model for the dynamics of self-propelled chemotactic microorganisms and illustrate it for the special case of a constant external chemotactic field in Sec. II B. The autochemotactic field is modeled in Sec. II C. A short summary of pure rotational diffusion in absence of chemotactic

 

interactions is presented in Sec. II D. Section II E shortly generalizes our model to an ensemble of autochemotactic walkers. In Sec. III we derive analytic expressions for the long-time diffusion coefficient of a single walker and confirm the findings numerically. Finally, we summarize our results in Sec. IV and provide an outlook, where we describe possible extensions of our model.

## II. MODEL OF THE AUTOCHEMOTACTIC WALKER

### A. Dynamic equation for the velocity direction

We model the time evolution of single trajectories of microorganisms that only move in two dimensions. The two-dimensional approach is justified because, aside from swimming, various forms of bacterial motility occur on surfaces [27]. The stochasticity in the motion of microorganisms is apparent [28]. An effective description therefore includes random forces and torques. Contributions to the stochastic terms originate from biochemical processes within a cell, e.g., when a cell detects and reacts to a chemical field, as well as from stochastic interactions of the microorganisms with their environment. An example of the latter is ordinary thermal noise, which leads to Brownian motion of a micron-sized colloid and originates from collisions with the much smaller fluid particles. However, in our case we cannot assume the fluctuation-dissipation theorem for the noise [29]. Note that our model particles should not be considered as swimming microorganisms since they move on a surface. Nevertheless, including details of the propulsion mechanism lies beyond the scope of our coarse-grained approach.

In two dimensions we write the velocity vector $\mathbf{v}(t)$ of a bacterium at time $t$ in polar coordinates, specified by the absolute value, the speed $v(t) \geqslant 0$, and the angle $\varphi(t) \in (-\pi,\pi]$ relative to the $x$ axis:

$$\mathbf{v}(t) = v(t) \begin{pmatrix} \cos\varphi(t) \\ \sin\varphi(t) \end{pmatrix}. \tag{1}$$

Experiments have demonstrated for different kinds of cells like granulocytes, monocytes, or fibroblasts that the functions $v(t)$ and $\varphi(t)$ are independent of each other [30]. Though this property has to be checked for each experimental setup, it is reasonable to assume it [31]. In addition, we will make the simplifying assumption that the speed $v$ of our model particle is constant. In contrast to the fast fluctuating stochastic variable of the velocity direction, the speed is a slow stochastic variable. As long as the microorganisms have a sufficiently large energy supply that enables them to move there exists a speed distribution with a pronounced mean [32–34]. In the case of granulocytes this distribution was even found to be Gaussian [30]. The motility of *E. coli* bacteria is determined by the well-known "run-and-tumble" dynamics, i.e., the alternating sequences of "run" and "tumbling" processes: During a "run" the bacterium moves along a nearly straight line with almost constant speed, whereas "tumbling" results in the random reorientation of the velocity direction [35]. In summary, expressing the velocity vector in polar coordinates seems to be the natural choice for describing the motion of microorganisms. In contrast, most models for chemotactic bacteria have used Cartesian velocity components [15,16,36,37].

In the following we derive the equation of motion for the velocity direction of a single microorganism in response to chemotaxis. The shape of our microorganism is arbitrary, e.g., spherical or rodlike. However, the particle is polar and possesses an intrinsic direction of motion that is characterized by a unit vector $\mathbf{e}$, e.g., parallel to its long axis. Furthermore, we assume that the particle always moves along this direction, so that $\mathbf{v}(t) = v\,\mathbf{e}(t)$. Though this connection between velocity direction and particle orientation seems rather evident for an isolated microorganism, it is no longer valid in a suspension of microorganisms as a consequence of hydrodynamic interactions [38].

To account for chemotaxis, we introduce the potential

$$V(\mathbf{e}) = -\mathbf{e}\cdot\mathbf{E}. \tag{2}$$

It aligns the velocity direction $\mathbf{e}$ with the chemotactic field $\mathbf{E}$ that is detected at the surface of the microorganism [39,40]. We will specify this chemotactic field in Sec. II C as the concentration gradient of a chemical. In microfluidic devices, the chemotactic field $\mathbf{E}$ is imposed externally [41,42]. For a wide range of bacterial strains the guiding field $\mathbf{E}$ is realized by various stimuli. Whereas for chemotaxis the stimulus is a chemical substance, galvanotaxis refers to electric fields, phototaxis to light, and thermotaxis to temperature [4]. Hence, in Eq. (2) $\mathbf{E}$ describes the guiding field for any kind of taxis.

Some microorganisms use a spatial sensing mechanism to detect the gradient of a chemical field instantaneously without performing a temporal average. It is primarily found in eukaryotic cells but in bacteria as well [43,44]. By applying the rotational operator $\mathcal{R} \equiv \mathbf{e} \times \frac{\partial}{\partial \mathbf{e}}$ to the chemotactic potential of Eq. (2) [45], one arrives at the chemotactic torque $\mathbf{M}_{\text{ext}} = -\mathcal{R}V(\mathbf{e}) = \mathbf{e} \times \mathbf{E}$ that acts on the velocity direction $\mathbf{e}$.

We now derive the dynamic equation for $\mathbf{e}(t)$ using Newton's equation of motion for the angular momentum $\mathbf{L}$,

$$\frac{\mathrm{d}}{\mathrm{d}t}\mathbf{L} = -\gamma_{\mathrm{R}}\boldsymbol{\Omega} + \mathbf{M}_{\text{ext}} + \boldsymbol{\Gamma}(t), \tag{3}$$

and the kinematic relation

$$\frac{\mathrm{d}}{\mathrm{d}t}\mathbf{e} = \boldsymbol{\Omega} \times \mathbf{e}, \tag{4}$$

which connects the angular velocity $\boldsymbol{\Omega}$ to $\mathbf{e}$. In Eq. (3) we have introduced a frictional torque $-\gamma_{\mathrm{R}}\boldsymbol{\Omega}$ where $\gamma_{\mathrm{R}} > 0$ is the rotational friction coefficient. The stochastic torque $\boldsymbol{\Gamma}(t)$ is modeled as Gaussian white noise whose Cartesian components are independent of each other. Its noise strength will be specified below.

Similar to swimming microorganisms that move at low Reynolds numbers, we will also work in the overdamped limit and neglect inertial terms [46]. This corresponds to Aristotelian dynamics where any motion immediately stops when forces and torques are not applied. The dimensionless Reynolds number Re compares inertial to viscous forces. Typical values for swimming microorganisms in water are $\mathrm{Re} \approx 10^{-5} - 10^{-4}$ for bacteria such as *E. coli*, $\mathrm{Re} \approx 10^{-2}$ for human spermatozoa, and up to $\mathrm{Re} \approx 10^{-1}$ for larger microorganisms like ciliates [46].

We therefore employ the Debye approximation [47], which neglects the inertial term in Eq. (3). Taking the cross product of Eq. (3) with $\mathbf{e}$, eliminating $\boldsymbol{\Omega}$ with Eq. (4), and using

$\mathbf{M}_{\rm ext} \times \mathbf{e} = (\mathbf{e} \times \mathbf{E}) \times \mathbf{e} = (\mathbb{1} - \mathbf{e} \otimes \mathbf{e})\,\mathbf{E}$, we arrive at a Langevin equation with multiplicative noise, still valid in two and three dimensions,

$$\frac{\mathrm{d}}{\mathrm{d}t}\,\mathbf{e} = \frac{1}{\gamma_{\rm R}}\,(\mathbb{1} - \mathbf{e} \otimes \mathbf{e})\,\mathbf{E} + \frac{1}{\gamma_{\rm R}}\,\mathbf{\Gamma}(t) \times \mathbf{e}, \tag{5}$$

where $\mathbb{1}$ denotes the unit matrix and $\otimes$ specifies the dyadic product. To formulate Eq. (5) in two dimensions, we parametrize the unit vector $\mathbf{e}$ by $\mathbf{e} = (\cos\varphi, \sin\varphi, 0)^T$ and let both $\mathbf{M}_{\rm ext}$ and $\mathbf{\Gamma}(t) = [0,0,\Gamma(t)]^T$ point along the $z$ axis. We still have to choose an interpretation of the stochastic differential equation (5) to give it a well-defined meaning (see Refs. [48,49] for mathematical details). We employ the Stratonovich interpretation since the Gaussian white noise approximates real colored noise with finite correlation time [48]. As a practical consequence, the common rules of classical calculus apply. In particular, we have $\frac{\mathrm{d}}{\mathrm{d}t}\,\mathbf{e} = \dot{\varphi}\,(-\sin\varphi, \cos\varphi, 0)^T$. With $\mathbf{E} = (E_x, E_y, 0)^T$, Eq. (5) becomes

$$\begin{pmatrix} -\sin\varphi \\ \cos\varphi \end{pmatrix} \dot{\varphi} = \frac{1}{\gamma_{\rm R}} \begin{pmatrix} \sin^2\varphi\; E_x - \sin\varphi\cos\varphi\; E_y \\ -\sin\varphi\cos\varphi\; E_x + \cos^2\varphi\; E_y \end{pmatrix} + \frac{1}{\gamma_{\rm R}}\,\Gamma(t) \begin{pmatrix} -\sin\varphi \\ \cos\varphi \end{pmatrix}, \tag{6}$$

from which a single Langevin equation for $\varphi(t)$ is immediately extracted. It only has additive noise due to the restriction to two dimensions. We assume that the mean of our Gaussian white noise is zero. Then we are able to write $\Gamma(t) = \gamma_{\rm R}\sqrt{2q_\varphi}\,\tilde{\Gamma}(t)$, where the positive constant $q_\varphi$ is the noise strength, and the scaled noise $\tilde{\Gamma}(t)$ has the properties that $\langle\tilde{\Gamma}(t)\rangle = 0$ and $\langle\tilde{\Gamma}(t)\tilde{\Gamma}(t')\rangle = \delta(t - t')$. Dropping again the tilde sign, we end up with

$$\frac{\mathrm{d}}{\mathrm{d}t}\,\varphi(t) = -\frac{E_x}{\gamma_{\rm R}}\,\sin\varphi(t) + \frac{E_y}{\gamma_{\rm R}}\,\cos\varphi(t) + \sqrt{2q_\varphi}\,\Gamma(t). \tag{7}$$

The chemotactic field $\mathbf{E}$ is a space- and time-dependent function. In particular, it depends on the position $\mathbf{r}(t) = [x(t), y(t)]^T$ of the autochemotactic walker, which is determined by integrating $\frac{\mathrm{d}}{\mathrm{d}t}\,\mathbf{r}(t) = \mathbf{v}(t) = v\mathbf{e}(t)$. We emphasize that the Langevin equation (7) consists of a deterministic part, which tries to align $\mathbf{e}(t)$ parallel to the chemotactic field, and a stochastic part, which causes rotational diffusion of the velocity direction. In Sec. II D some properties of pure rotational diffusion will be summarized by setting $\mathbf{E} = \mathbf{0}$.

Note that the deterministic part of Eq. (7) can also be derived by formulating the Euler-Lagrange equation for $\varphi(t)$ with the potential from Eq. (2) and the Rayleigh dissipation function $W = \frac{1}{2}\gamma_{\rm R}\dot{\varphi}^2$ [50]. In Ref. [51] Gruler and Franke have introduced a model with a more general potential $V(\mathbf{e},\mathbf{E})$. Our potential is the leading term in a Fourier expansion, linear in $\mathbf{E}$.

### B. Constant chemotactic field

To get familiar with Eq. (7), we first consider the special case of a constant field $\mathbf{E}$ in the absence of noise ($q_\varphi = 0$). A constant chemotactic field can be realized with microfluidic techniques [41]. With $\mathbf{E} = E\mathbf{e}_x$ ($E > 0$), Eq. (7) reads

$$\frac{\mathrm{d}}{\mathrm{d}t}\,\varphi(t) = -\frac{E}{\gamma_{\rm R}}\,\sin\varphi(t), \tag{8}$$

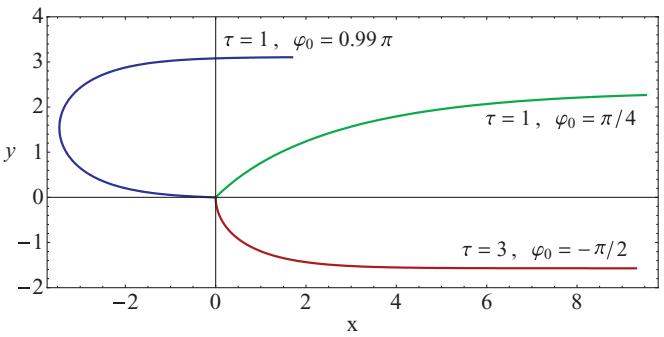


FIG. 1. (Color online) Plot in arbitrary units of three deterministic trajectories in the constant chemotactic field $\mathbf{E} = E\mathbf{e}_x$ according to Eq. (10). All particles have starting point $\mathbf{r}_0 = (0,0)$, speed $v = 1$, and move during the time interval $t \in [0,10]$.

which we solve by separation of variables,

$$\varphi(t) = 2\arctan[\tan(\varphi_0/2)\,e^{-t/\tau}], \tag{9}$$

with $\tau = \gamma_{\rm R}/E$. The walker starts with an angle $\varphi_0$ at $t = 0$. Its velocity direction relaxes toward the $x$ axis and aligns along $\mathbf{E}$ during the characteristic time $\tau$. Remarkably, using Eq. (9) in $\frac{\mathrm{d}}{\mathrm{d}t}\,\mathbf{r}(t) = v\mathbf{e}(t)$, one can determine the full trajectory analytically:

$$\begin{aligned} x(t) &= x_0 + vt + v\tau\,\ln\left[\frac{1 + \tan^2(\varphi_0/2)e^{-2t/\tau}}{1 + \tan^2(\varphi_0/2)}\right], \\ y(t) &= y_0 + 2v\tau\left\{\arctan\left[\frac{e^{t/\tau}}{\tan(\varphi_0/2)}\right] - \arctan\left[\frac{1}{\tan(\varphi_0/2)}\right]\right\}. \end{aligned} \tag{10}$$

This result confirms that in the long-time limit $t \gg \tau$ the particle walks in $x$ direction with speed $v$ while it asymptotically reaches a constant $y$ coordinate. Three trajectories for different initial angles $\varphi_0$ and relaxational times $\tau$ are presented in Fig. 1.

For completeness, we briefly discuss the consequences of the noise term $\sqrt{2q_\varphi}\,\Gamma(t)$ added to Eq. (8) [52]. For the resulting Langevin equation, we formulate the associated Fokker-Planck equation for the probability density function $P = P(\varphi,t)$ [29]:

$$\frac{\partial P}{\partial t} = \frac{1}{\tau}\,\frac{\partial}{\partial\varphi}\,(P\sin\varphi) + q_\varphi\,\frac{\partial^2}{\partial\varphi^2}\,P\,. \tag{11}$$

In the long-time limit, $P(\varphi,t)$ relaxes toward the stationary solution [29]

$$P_{\rm stat}(\varphi) = \frac{\exp\left(\frac{1}{q_\varphi\tau}\cos\varphi\right)}{2\pi\,I_0\left(\frac{1}{q_\varphi\tau}\right)}, \tag{12}$$

where the modified Bessel function of first kind $I_0$ has entered as a normalization factor. $P_{\rm stat}(\varphi)$ is the von Mises distribution and is also known as the circular normal distribution. It is reminiscent of the Boltzmann distribution of dipoles in an external field in thermal equilibrium. $P_{\rm stat}(\varphi)$ is symmetric around the origin with maximum at $\varphi = 0$ and decays to a finite value for $\varphi \to \pm\pi$ as shown in Fig. 2. We quantify the

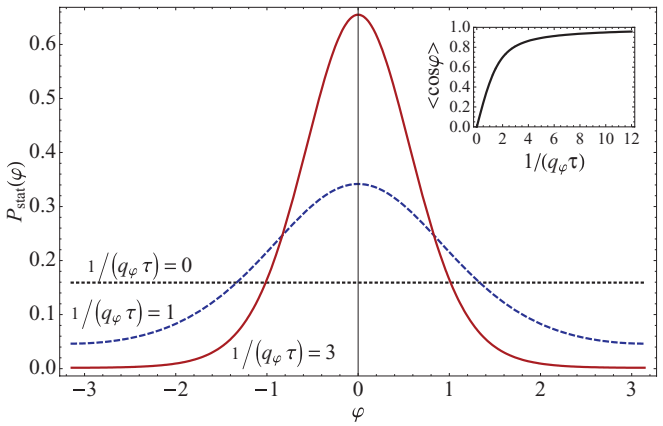


FIG. 2. (Color online) Stationary probability distribution for different chemotactic fields according to Eq. (12). For $E \propto \tau^{-1} = 0$, the distribution is constant. The inset shows the order parameter $\langle\cos\varphi\rangle$ as a function of $1/(q_\varphi\tau)$.

average alignment of the walker along the chemotactic field by the order parameter

$$\langle\cos\varphi\rangle = \int_{-\pi}^{+\pi} \mathrm{d}\varphi\, P_{\rm stat}(\varphi)\cos\varphi = \frac{I_1\left(\frac{1}{q_\varphi\tau}\right)}{I_0\left(\frac{1}{q_\varphi\tau}\right)}, \tag{13}$$

where $I_1$ denotes the modified Bessel function of first kind. For strong chemotactic fields or weak noise, $\tau \ll 1/q_\varphi$, the order parameter approaches one (inset of Fig. 2), and the velocity vector is completely oriented parallel to the external field. For a small chemotactic field, $\tau \gg 1/q_\varphi$, the order parameter increases linearly in $1/(q_\varphi\tau)$. The average drift velocity becomes $\mathbf{v}_{\rm drift} = v\,\langle\cos\varphi\rangle\,\mathbf{e}_x$, which vanishes for $\mathbf{E} = \mathbf{0}$ due to the rotational diffusion of the walker.

### C. Chemotactic field of the autochemotactic walker

Next, we model the chemotactic field, which is self-consistently generated by the walker itself. The walker or bacterium secretes a chemical substance with a constant production rate $h$. We assume that the chemical spreads through the environment by classical diffusion, with diffusion constant $D_c$. Due to enzymatic activity in the environment, the chemical also decays with a rate $k$, which we assume constant for simplicity. The concentration field of the chemical thus obeys the reaction diffusion equation

$$\frac{\partial}{\partial t}\,c(\mathbf{r},t) = D_c\nabla^2 c - kc + h\rho, \tag{14}$$

where $\rho(\mathbf{r},t) = \delta[\mathbf{r} - \mathbf{r}_a(t)]$ is the density of the walker with trajectory $\mathbf{r}_a(t)$ and $\nabla^2$ is the Laplacian in two dimensions.

Assuming that the walker starts to produce the chemical at $t = 0$, the solution of Eq. (14) is the Green function integrated over all positions $\mathbf{r}_a(t')$ of the walker:

$$c(\mathbf{r},t) = \frac{h}{4\pi D_c}\int_0^t \mathrm{d}t'\,\frac{e^{-k(t-t')}}{t-t'}\exp\left(-\frac{[\mathbf{r}-\mathbf{r}_a(t')]^2}{4D_c(t-t')}\right). \tag{15}$$

This result reveals the non-Markovian character of our system since the concentration at time $t$ is influenced by the walker's position at times $t' < t$. The numerical evaluation of the integral is, however, facilitated as the exponential decay admits to reduce the integration range to times $t'$ with $k(t-t') \lesssim 1$. We note that Eq. (14) was already suggested in the basic version of the Keller-Segel model (with a continuous density $\rho$). It is also found in recent chemotaxis models [15,19,37,53,54].

The chemotactic field is now proportional to the gradient of the chemical:

$$\mathbf{E}(\mathbf{r},t) = \kappa(c)\,\nabla c(\mathbf{r},t). \tag{16}$$

The chemotactic factor or chemotactic sensitivity $\kappa(c)$ determines the coupling strength, and its sign enables one to distinguish between positive (attractive) and negative (repulsive) chemotaxis. For $\kappa(c)$ a plethora of possible forms has been proposed [13]. Prominent examples that confine the chemotactic field for increasing concentration are the "logarithmic response" $\kappa(c) = A/c$ or the "receptor law" $\kappa(c) = A/(B+c)^2$ with positive constants $A$, $B$. In this publication, we consider the simplest case of a constant coupling strength $\kappa(c) = \kappa$. The chemotactic field entering the Langevin equation (7) for the walker's velocity direction is therefore given by $\mathbf{E}(\mathbf{r},t) = \kappa\nabla c(\mathbf{r},t)$, evaluated at the walker's position $\mathbf{r}_a(t)$.

The integrand in Eq. (15) diverges at the upper bound. Therefore we introduce a regularization time $\tau_{\rm del} > 0$ such that the upper bound changes to $t - \tau_{\rm del}$ [16]. One can justify $\tau_{\rm del}$ as the delay time before the microorganism starts to feel the chemical. In our numerical simulations, we do not regard $\tau_{\rm del}$ as a relevant parameter of our model and set it to the value of the time step. Finally, we point out that there are other alternatives to circumvent the introduction of $\tau_{\rm del}$ when evaluating the concentration $c(\mathbf{r}_a(t),t)$ at the cell's position, for instance, by taking the finite size of the cell into account.[1]

### D. Pure rotational diffusion

In the absence of a chemotactic field, the walker performs pure rotational diffusion:

$$\frac{\mathrm{d}}{\mathrm{d}t}\,\varphi(t) = \sqrt{2q_\varphi}\;\Gamma(t). \tag{17}$$

With help of the corresponding diffusion equation for the angular probability density, $\partial_t p = q_\varphi\partial_\varphi^2 p$, one calculates the directional correlation function [45]

$$\langle\mathbf{e}(t)\cdot\mathbf{e}(t')\rangle = e^{-q_\varphi|t-t'|}. \tag{18}$$

On the time scale $\tau_{\rm rot} = q_\varphi^{-1}$, directional correlations decay to zero. In contrast, for $|t-t'| \ll \tau_{\rm rot}$ the random walker is persistent and moves into the same direction for a persistence length $s_{\rm per} = v\tau_{\rm rot}$. For constant speed $v$, the mean-squared displacement yields (see, e.g., Ref. [31])

$$\langle[\mathbf{r}_a(t) - \mathbf{r}_a(0)]^2\rangle = \frac{2v^2}{q_\varphi^2}\,(q_\varphi t - 1 + e^{-q_\varphi t}), \tag{19}$$

from which we extract the diffusion coefficient

$$D = \lim_{t\to\infty}\frac{\langle[\mathbf{r}_a(t) - \mathbf{r}_a(0)]^2\rangle}{4t} = \frac{v^2}{2q_\varphi}. \tag{20}$$

[1] One could represent the cell's observed concentration by the convolution of $c(\mathbf{r},t)$ with a Gaussian filter whose width is comparable to the cell size.

A Taylor expansion of Eq. (19) for $q_\varphi t \ll 1$ gives the ballistic motion for small times.

### E. Generalization to an ensemble of autochemotactic walkers

The model introduced so far can easily be generalized to many autochemotactic walkers. In a system of $m$ individuals, the $i$th walker is characterized by its velocity direction $\mathbf{e}_i(t) = [\cos\varphi_i(t),\ \sin\varphi_i(t)]^T$ and position $\mathbf{r}_i(t)$ that is obtained by integrating $\frac{\mathrm{d}}{\mathrm{d}t}\mathbf{r}_i(t) = \mathbf{v}_i(t) = v\mathbf{e}_i(t)$. The angle $\varphi_i(t)$ obeys the Langevin equation (7), where the Gaussian white noise $\Gamma_i(t)$ of different particles is uncorrelated, $\langle\Gamma_i(t)\Gamma_j(t')\rangle = \delta_{ij}\delta(t-t')$. The chemotactic field $\mathbf{E}(\mathbf{r},t) = \kappa\nabla c(\mathbf{r},t)$ mediates an interaction between the walkers. It is determined from the reaction diffusion equation (14) using the particle density $\rho(\mathbf{r},t) = \sum_{i=1}^{m}\delta[\mathbf{r}-\mathbf{r}_i(t)]$. As all microorganisms contribute to the production of the chemical, our model of autochemotaxis introduces a communication mechanism or signaling between the cells [1]. In the case of attractive autochemotaxis, cluster formation can be observed [55].

## III. LONG-TIME DIFFUSION COEFFICIENT OF THE AUTOCHEMOTACTIC WALKER

In the following we consider a single autochemotactic walker that moves in its self-generated cloud of chemical. Even for this one-particle problem the non-Markovian property does not allow a full analytic treatment. We can, however, find an analytic expression for the walker's mean-squared displacement for large times, and thereby extract the effective diffusion coefficient $D_{\mathrm{eff}}$. We will calculate $D_{\mathrm{eff}}$ analytically for weak (Sec. III A) and strong (Sec. III B) chemotactic coupling and then compare to numerical simulations in Sec. III C.

### A. Weak chemotactic coupling

In the following, we perform an approximate treatment of the chemotactic walker, for which we will show at the end that it is only valid for sufficiently small chemotactic coupling. Our treatment is motivated by the work of Grima in Ref. [19]. After substituting $t - t' = ut$, the gradient of Eq. (15), evaluated at the walker's position $\mathbf{r}_a(t)$, reads

$$\nabla c(\mathbf{r}_a(t),t) = -\frac{h}{8\pi D_c^2}\,\frac{1}{t}\int_{\tau_{\mathrm{del}}/t}^{1}\mathrm{d}u\,\frac{\mathbf{r}_a(t)-\mathbf{r}_a(t-ut)}{u^2} \times \exp\left(-\frac{[\mathbf{r}_a(t)-\mathbf{r}_a(t-ut)]^2}{4D_c t u} - ktu\right). \tag{21}$$

This expression cannot be evaluated in general. However, as we are interested in the mean-squared displacement for large times $t \gg 1/k$, we perform an asymptotic analysis with $kt \gg 1$. The integral in Eq. (21) is then dominated by the exponential function calculated at $u \ll 1$. With the Taylor expansion up to second order in $u$,

$$\mathbf{r}_a(t) - \mathbf{r}_a(t-ut) = ut\dot{\mathbf{r}}_a(t) - \frac{(ut)^2}{2}\ddot{\mathbf{r}}_a(t) + \mathcal{O}(u^3), \tag{22}$$

we calculate

$$[\mathbf{r}_a(t) - \mathbf{r}_a(t-ut)]^2 = (vut)^2 + \mathcal{O}(u^4). \tag{23}$$

Here we used $\dot{\mathbf{r}}_a = v\mathbf{e}$, $\mathbf{e}^2 = 1$, and $\dot{\mathbf{r}}_a\cdot\ddot{\mathbf{r}}_a = v^2\mathbf{e}\cdot\dot{\mathbf{e}} = 0$. In contrast to Grima's model in Ref. [19], we will need the second-order term in Eq. (22) for further analysis. We use Eqs. (22) and (23) to expand $\nabla c(\mathbf{r}_a(t),t)$ from Eq. (21) up to second order in $u$ and derive from Eq. (7) a Langevin equation for the velocity direction, valid at large times,

$$\frac{\mathrm{d}}{\mathrm{d}t}\varphi(t) = \sqrt{2q_\varphi^{\mathrm{eff}}}\,\Gamma(t) \tag{24}$$

with

$$q_\varphi^{\mathrm{eff}} = q_\varphi/f_{\mathrm{ch}},\quad f_{\mathrm{ch}} = \left(1 - \frac{\kappa h v\exp(-\zeta\tau_{\mathrm{del}})}{16\pi\gamma_{\mathrm{R}}D_c^2\zeta}\right)^2 \tag{25}$$

and $\zeta = v^2/(4D_c) + k$. Details of the derivation are presented in Appendix A. Equation (24) shows that in the long-time limit the particle performs diffusive motion with the effective diffusion coefficient

$$D_{\mathrm{eff}} = \frac{v^2}{2q_\varphi^{\mathrm{eff}}} = \frac{v^2}{2q_\varphi}\,f_{\mathrm{ch}}. \tag{26}$$

Note that even in the limit for vanishing delay time $\tau_{\mathrm{del}} \to 0$ the expression for $D_{\mathrm{eff}}$ remains finite.

In Sec. III C we will present numerical investigations in unitless quantities by using characteristic quantities of the diffusing chemical. We rescale time by the inverse decay rate, $t_c = 1/k$, and length by $l_c = \sqrt{D_c/k}$, the distance the chemical diffuses during its lifetime $t_c$. Our rescaled model then contains three essential parameters: The effective chemotaxis strength

$$\Lambda = h\kappa\,\frac{t_c^2}{\gamma_{\mathrm{R}}l_c^3} \tag{27}$$

is proportional to coupling constant $\kappa$ and production rate $h$, the noise strength $\tilde{q}_\varphi = q_\varphi t_c$, and the speed of the walker $\tilde{v} = vt_c/l_c$. In addition, the rescaled delay time is $\tilde{\tau}_{\mathrm{del}} = \tau_{\mathrm{del}}/t_c$. The diffusion coefficient $\tilde{D}_{\mathrm{eff}} = \tilde{v}^2/(2\tilde{q}_\varphi^{\mathrm{eff}})$ is measured in units of the chemical's diffusion coefficient $D_c = l_c^2\,t_c^{-1}$. In the following, we will drop all the tilde signs to ease the notation. Then the rescaled diffusion coefficient from Eq. (26) becomes

$$D_{\mathrm{eff}} = \frac{v^2}{2q_\varphi}\left(1 - \frac{\Lambda}{16\pi}\,\frac{v}{1+v^2/4}\,e^{-(1+v^2/4)\tau_{\mathrm{del}}}\right)^2. \tag{28}$$

For large delay times $\tau_{\mathrm{del}} \gg 1$, the diffusion coefficient (28) equals the free diffusion coefficient $D = \frac{v^2}{2q_\varphi}$, since the chemical has already decayed to zero before the walker reacts on it. Also, for $v \gg 1$, we find $D_{\mathrm{eff}} = D$, since the particle moves faster than the diffusive spread of its own chemotactic field.

In the case of large attractive or repulsive chemotactic coupling, Eq. (28) predicts a quadratic scaling $D_{\mathrm{eff}} \propto |\Lambda|^2$. For negative autochemotaxis this result is conceivable, whereas it is obviously wrong for attractive chemotaxis since a strong attraction of the particle by its own secretion should reduce the diffusion coefficient. We therefore have to restrict the validity of Eq. (28) to $\Lambda < \Lambda_0$, where

$$\Lambda_0 = 16\pi\,\frac{1+v^2/4}{v}\,e^{(1+v^2/4)\tau_{\mathrm{del}}} \tag{29}$$

is the coupling constant with $D_{\rm eff} = 0$. Indeed, for $0 < \Lambda < \Lambda_0$, $D_{\rm eff}$ decreases with increasing $\Lambda$, as expected. The validity of Eq. (28) breaks down for large $\Lambda$ since in Eqs. (22) and (23) we neglected higher-order terms in $u$ when calculating the chemotactic field. This will become clearer in the next subsection.

### B. Strong chemotactic coupling

To treat the case of strong chemotactic coupling, we rewrite the Langevin equation (7) as

$$\frac{\mathrm{d}}{\mathrm{d}t}\,\varphi(t) = \Omega(t) + \sqrt{2q_\varphi}\,\Gamma(t), \tag{30}$$

where the time-dependent frequency or angular drift velocity $\Omega(t)$ is given by

$$\Omega(t) = -\frac{E_x(\mathbf{r}_a(t),t)}{\gamma_{\rm R}}\,\sin\varphi(t) + \frac{E_y(\mathbf{r}_a(t),t)}{\gamma_{\rm R}}\,\cos\varphi(t). \tag{31}$$

We now consider a sufficiently strong attractive chemotactic field and neglect noise for a moment. The walker emits the chemical and thereby creates a concentration gradient opposite to the direction of motion, with which the walker always tries to align. Hence for strong positive chemotaxis, we expect circular trajectories with a constant circling frequency $\Omega(t) = \omega$. This scenario is confirmed as the trajectory on the left of Fig. 3 demonstrates. One might have expected that for strong chemotactic coupling the walker rests in the center of a stationary concentration profile. However, this is not possible since the self-propelled particle always moves with constant speed.

In the following we calculate the circling frequency $\omega$ self-consistently for $q_\varphi = 0$. We describe the circular trajectory of the walker around the origin by

$$\mathbf{r}_a(t) = r_0 \begin{pmatrix} \sin\omega t \\ -\cos\omega t \end{pmatrix}, \tag{32}$$

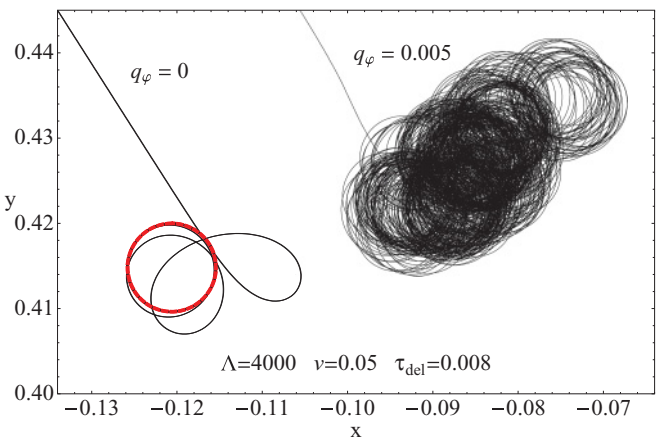


FIG. 3. (Color online) Trajectories for strong attractive chemotaxis simulated with the full model of Eq. (7) or (30). Left: Deterministic motion ($q_\varphi = 0$) toward a limit cycle (shown as circle in bold line). Right: With noise ($q_\varphi = 0.005$) the circular motion is perturbed and the circle's center diffuses.

where $r_0$ is the radius and positive or negative $\omega$ leads to anticlockwise or clockwise circling, respectively. The velocity reads

$$\mathbf{v}(t) = \dot{\mathbf{r}}_a(t) = v \begin{pmatrix} \cos\varphi(t) \\ \sin\varphi(t) \end{pmatrix}, \tag{33}$$

with

$$\varphi(t) = \omega t \quad \text{and} \quad v = r_0\omega, \tag{34}$$

consistent with our model. After substituting Eq. (32) into the chemotactic field $\mathbf{E} = \mathbf{E}(\mathbf{r}_a(t),t) = \kappa\,\nabla c(\mathbf{r}_a(t),t)$ with $c$ from Eq. (15) and using some trigonometric identities, we obtain

$$\mathbf{E} = -\frac{\kappa h r_0}{4\pi D_c^2}\int_0^{t-\tau_{\rm del}} \mathrm{d}t'\,\frac{e^{-k(t-t')}}{(t-t')^2}\,\sin\left[\frac{\omega}{2}(t-t')\right] \times \begin{pmatrix} \cos[\frac{\omega}{2}(t+t')] \\ \sin[\frac{\omega}{2}(t+t')] \end{pmatrix} \exp\left(-\frac{r_0^2\sin^2\left[\frac{\omega}{2}(t-t')\right]}{D_c(t-t')}\right). \tag{35}$$

Then we insert Eq. (35) into Eq. (31), set $\Omega(t) = \omega$, and employ Eq. (34). We introduce again our reduced variables, in particular the effective chemotactic coupling strength $\Lambda$, and after substituting $t - t'$ by $ut$ we arrive at

$$1 = \frac{\Lambda v}{4\pi\omega^2}\int_{\tau_{\rm del}/t}^1 \mathrm{d}u\,\frac{1}{t}\,\frac{e^{-tu}}{u^2}\,\sin^2\left(\frac{\omega t}{2}u\right) \times \exp\left[-\frac{v^2}{\omega^2}\,\frac{\sin^2\left(\frac{\omega t}{2}u\right)}{tu}\right]. \tag{36}$$

This is an implicit equation for the unknown circling frequency $\omega$ valid at large times. Note that at short times the particle has not yet reached the circling motion. It is possible to solve Eq. (36) numerically for $\omega = \omega(\Lambda, v, \tau_{\rm del}; t)$. For $t \to \infty$ we can also calculate the integral in Eq. (36) analytically since the exponential in the second line becomes one, the lower bound of the integral tends to zero, and the upper bound can be set to infinity due to $e^{-tu}$. Evaluating the resulting integral yields

$$1 \approx \frac{\Lambda v}{4\pi\omega^2}\left[\frac{\omega}{2}\,\arctan\omega - \frac{1}{4}\,\ln(1+\omega^2)\right], \tag{37}$$

independent of the delay time $\tau_{\rm del}$. From Eq. (37) we derive a necessary condition for a solution $\omega$ to exist:[2]

$$\Lambda \gtrsim \frac{16\pi}{v}, \tag{38}$$

which we confirm by simulations in Sec. III C. Comparing this lower bound for $\Lambda$ to Eq. (29) shows that the range of validity is complementary to the case of weak coupling.

We now include noise of strength $q_\varphi$ in Eq. (30). As the trajectory on the right of Fig. 3 demonstrates, this perturbs the

[2]A solution $\omega$ satisfies $\frac{4\pi}{\Lambda v}\,\omega^2 = \frac{\omega}{2}\,\arctan\omega - \frac{1}{4}\,\ln(1+\omega^2)$. For large $\omega$, the dominant term of the right-hand side behaves as $\propto \frac{\pi}{2}\omega - \frac{1}{2}\ln\omega$. The leading term is thus linear in $\omega$ and therefore the function $\frac{\omega}{2}\,\arctan\omega - \frac{1}{4}\,\ln(1+\omega^2)$ lies below the parabola $\frac{4\pi}{\Lambda v}\,\omega^2$ on the left-hand side. For a solution to exist, both functions have to intersect, and for small $\omega$ the relation $\frac{4\pi}{\Lambda v}\,\omega^2 < \frac{\omega}{2}\,\arctan\omega - \frac{1}{4}\,\ln(1+\omega^2)$ has to be fulfilled. With the Taylor expansion $\frac{\omega^2}{4}$ for the right-hand side, we obtain $\frac{4\pi}{\Lambda v} < \frac{1}{4}$.

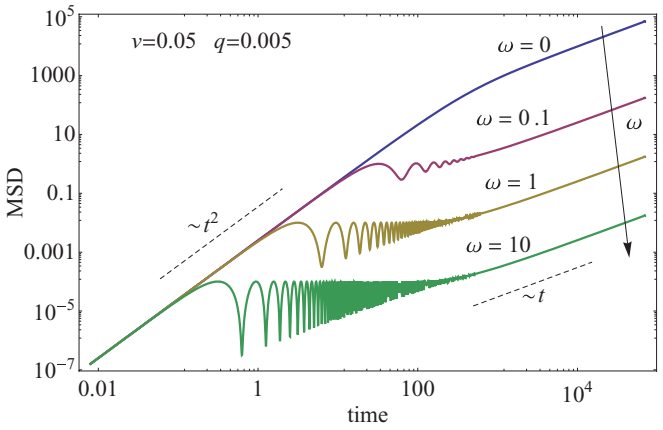


FIG. 4. (Color online) Mean-squared displacement (MSD) of a circling particle with noise according to Eq. (40) for different frequencies $\omega$. Speed $v$ and noise strength $q$ are fixed.

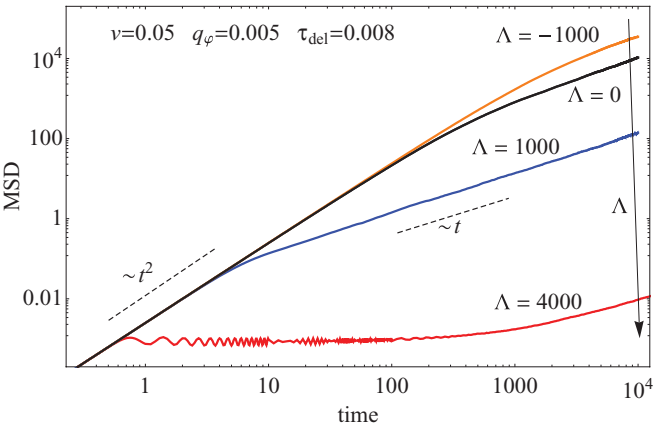


FIG. 5. (Color online) MSD as a function of time for different effective chemotaxis strengths $\Lambda$ obtained by simulating the full model of Eq. (7). Negative $\Lambda$ correspond to repulsive chemotaxis; positive $\Lambda$ are due to a chemoattractant.

perfect circular motion of the walker. Since $\varphi(t)$ but also the chemotactic field $\mathbf{E}(\mathbf{r}_a(t),t)$ become fluctuating quantities, the angular drift velocity in Eq. (31) also fluctuates around $\omega$: $\Omega(t) = \omega + \delta\omega(t)$. In Sec. III C we will demonstrate that the fluctuations $\delta\omega(t)$ are Gaussian distributed so that we can replace them by an additional noise strength $q_\omega$. We therefore generalize $\frac{\mathrm{d}}{\mathrm{d}t}\varphi(t) = \omega$ by adding Gaussian white noise of strength $q = q_\varphi + q_\omega$:

$$\frac{\mathrm{d}}{\mathrm{d}t}\varphi(t) = \omega + \sqrt{2q}\,\Gamma(t). \tag{39}$$

In Appendix B we calculate the mean-squared displacement (MSD) using Eq. (39):

$$\begin{aligned}\langle[\mathbf{r}_a(t) - \mathbf{r}_a(0)]^2\rangle \\ = \frac{2v^2qt}{q^2+\omega^2} - \frac{2v^2(q^2-\omega^2)}{(q^2+\omega^2)^2} + \frac{2v^2e^{-qt}}{(q^2+\omega^2)^2} \\ \times[(q^2-\omega^2)\cos(\omega t) - 2q\omega\sin(\omega t)].\end{aligned} \tag{40}$$

Figure 4 shows a double-logarithmic plot of the MSD. Initially, the walker moves ballistically, and then the MSD starts to oscillate when the walker performs its full circular motion.

TABLE I. Characteristic parameters in real units for *E. coli* and *Dicty* [58–61]. Chemoattractants of *E. coli* are sugars or amino acids, their decay rate $k$ is estimated. The chemoattractant of *Dicty*, cAMP, is degraded by phosphodiesterase (PDE). The directional correlation time $\tau_{\mathrm{rot}}$ of *E. coli* is adjusted such that it gives the measured diffusion coefficient $D = v^2/(2q_\varphi)$. It equals the duration of three run-and-tumble events. Other values are calculated from $s_{\mathrm{per}} = v/q_\varphi$ and $l_c = \sqrt{D_c/k}$.

| | size [$\mu$m] | $v$ [$\mu$m/s] | $\tau_{\mathrm{rot}} = q_\varphi^{-1}$ [s] | $D$ [m$^2$/s] | |
|---|---|---|---|---|---|
| *E. coli* | 1 . . . 2 | 20 | 3.3 | $6.6\times10^{-10}$ | |
| *Dicty* | 8 . . . 12 | 0.1 | 500 | $2.5\times10^{-12}$ | |
| $s_{\mathrm{per}}$ [$\mu$m] | $D_c$ [m$^2$/s] | $D/D_c$ | $k$ [1/s] | $l_c$ [$\mu$m] | $s_{\mathrm{per}}/l_c$ |
| 66 | $10^{-9}$ | 0.66 | 10 | 10 | 6.6 |
| 50 | $3\times10^{-10}$ | 0.01 | 0.09 | 67 | 0.7 |

This is confirmed by taking the short-time limit of Eq. (40) for $\omega \gg q$ at $t \ll q^{-1}$: $\langle[\mathbf{r}_a(t) - \mathbf{r}_a(0)]^2\rangle \approx \frac{4v^2}{\omega^2}[\sin^2(\frac{\omega}{2}t) + qt\cos^2(\frac{\omega}{2}t)]$. Finally, at large times, the walker diffuses with an effective diffusion coefficient

$$D_{\mathrm{eff}} = D_{\mathrm{eff}}(q,\omega) = \frac{v^2}{2q}\,\frac{1}{1+\left(\frac{\omega}{q}\right)^2}. \tag{41}$$

It is written as a product of the free diffusion coefficient and the Cauchy-Lorentz function with variable $\omega/q$. For fixed $q$, $D_{\mathrm{eff}}$ is maximal for $\omega = 0$, i.e., in the absence of any circling. For given $\omega$, the maximal diffusion coefficient is at $q = |\omega|$. So, the diffusion coefficient, as the system's response to noise, is maximal for a nonzero $q$. This resembles stochastic resonance, where a weak signal is amplified by noise of certain strength.

### C. Comparison of analytical and numerical results

To check our predictions, we perform simulations of the full model in Eq. (7) in reduced units by averaging over at least 1000 different realizations of noise for each set of parameters. In Table I we list typical experimental or estimated values for the parameters of the paradigmatic organisms *E. coli* and *Dictyostelium discoideum* (*Dicty*). We adjust our reduced parameters introduced in Sec. III A to agree with these experimental values. In particular, we choose $v = 0.05$ and $q_\varphi = 0.005$, which yields the free diffusion coefficient $D = v^2/(2q_\varphi) = 0.25$ and the persistence length $s_{\mathrm{per}} = v/q_\varphi = 10$.

In Fig. 5 we plot the MSD as a function of time without chemoattractant ($\Lambda = 0$), as well as for attractive ($\Lambda > 0$) and repulsive ($\Lambda < 0$) chemotaxis. For all values of $\Lambda$ we observe diffusive motion at large times, where the diffusion coefficient decreases with increasing coupling strength. The lowest curve in Fig. 5 reveals oscillations of the MSD[3] reminiscent of Fig. 4.

Figure 6 plots the diffusion coefficient $D_{\mathrm{eff}}$ versus the coupling strength $\Lambda$ for $\Lambda < \Lambda_0 \approx 1014$. The analytic expression

[3]The oscillations in the MSD for $\Lambda = 4000$ change abruptly since at time $t \gtrsim 10$ we change the time resolution of the graph.

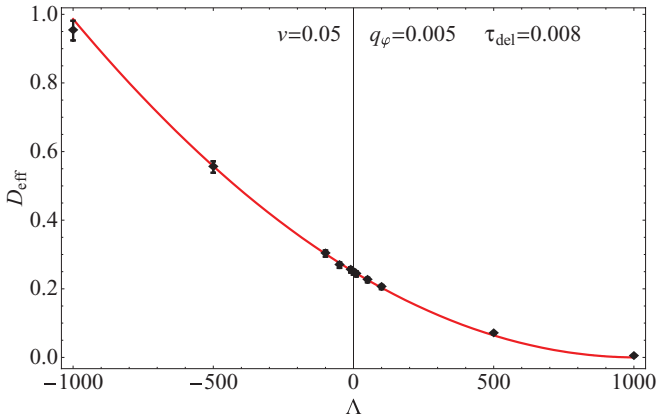


FIG. 6. (Color online) Diffusion coefficient as a function of effective chemotaxis strength Λ for weak coupling. The points with error bars are obtained by simulating the full model; the full line is expression (28).

for $D_{\rm eff}$ in Eq. (28) (full line in Fig. 6) agrees very well with the simulated values. Note that at $\Lambda \approx -1000$ $D_{\rm eff}$ becomes one. Since the massive microorganisms should diffuse slower than the molecules of the chemical [3,56,57], this restricts repulsive chemotaxis to $\Lambda > -1000$. We further checked our theory by confirming that the directional correlation function of Eq. (18) decays exponentially with the time constant $1/q_\varphi^{\rm eff}$ calculated from the effective noise strength of Eq. (25).

For large chemotactic coupling we employ the theory of Sec. III B, which according to Eq. (38) holds for $\Lambda > 16\pi/v \approx 1005$. Results from theory and simulations are compared in Fig. 7. When we approximate the effective noise strength $q$ of our strong-coupling model by the original noise $q_\varphi$, the diffusion coefficient $D_{\rm eff}$ is clearly too small (dashed line in Fig. 7). We already noted that with noise the angular drift velocity $\Omega(t)$ of the full model reformulated in Eqs. (30) and (31) becomes a fluctuating quantity. We present the time evolution of $\Omega(t)$ in Fig. 8. Without noise, $\Omega(t)$ readily converges to a constant value that agrees well with the theoretical value $\omega$ (dashed line in Fig. 8). With noise, $\Omega(t)$ fluctuates around

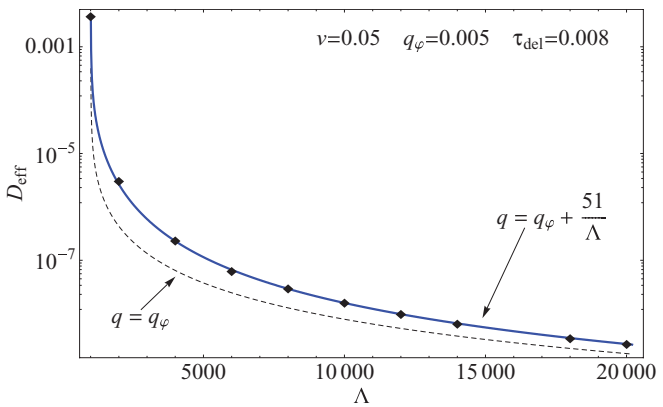


FIG. 7. (Color online) Diffusion coefficient as a function of large chemotaxis strength Λ. The dashed curve is the analytic expression (41) with the effective noise strength $q = q_\varphi$. The full line belongs to $q = q_\varphi + 51/\Lambda$. Data points are obtained by simulating the full model.

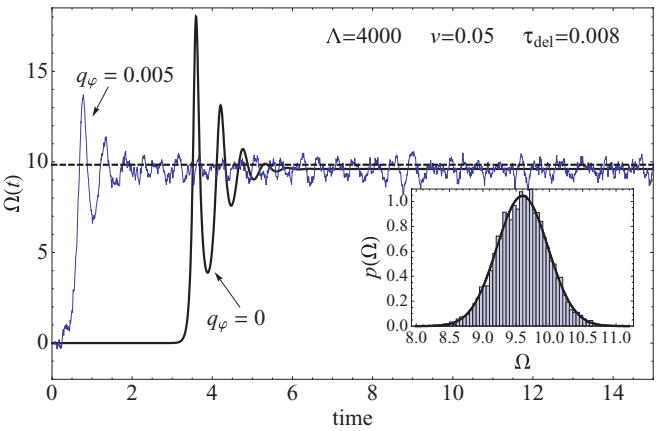


FIG. 8. (Color online) Angular drift velocity $\Omega(t)$ for chemotactic coupling $\Lambda = 4000$ as a function of time for $q_\varphi = 0$ (thick line). With noise of strength $q_\varphi = 0.005$, $\Omega(t)$ fluctuates. For comparison, the dashed line indicates the self-consistently determined $\omega$ from Eq. (37). The inset shows the distribution $p(\Omega)$ of $\Omega(t)$ values. It is well described by a Gaussian distribution (solid line).

a mean value close to $\omega$. The distribution $p(\Omega)$ plotted as inset in Fig. 8 identifies the angular drift velocity $\Omega(t)$ as Gaussian distributed. Thus the Gaussian distribution of the original noise $q_\varphi$ is inherited to the fluctuations of $\Omega(t)$. In our effective description of Eq. (39), we take them into account by an additional noise strength $q_\omega$ and the total noise becomes $q = q_\varphi + q_\omega$. As Fig. 7 demonstrates, the diffusion coefficient $D_{\rm eff}$ of Eq. (41) shows a striking agreement with simulations, when we choose

$$q_\omega = q_\omega(\Lambda) = c\,\Lambda^{-1}, \tag{42}$$

where $c \approx 51$ is a fit parameter. So far, we were not able to rigorously justify Eq. (42).

We add two remarks. First, at $\Lambda = 2000$ $q_\omega \approx 0.026$ exceeds the original noise strength $q_\varphi = 0.005$ by a factor of 5 and therefore determines the total noise $q$. Second, $D_{\rm eff}$ increases with increasing noise $q$ since in Eq. (41) we evaluate $D_{\rm eff}$ at $\omega \gg q_\varphi$.

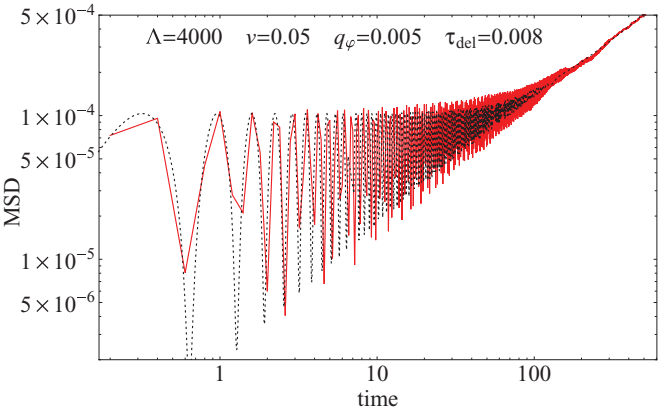


FIG. 9. (Color online) MSD for strong chemotactic coupling $\Lambda = 4000$. The solid line is obtained numerically from simulations of the full model of Eq. (7), and the dashed curve corresponds to Eq. (40) with noise strength $q = q_\varphi + 51/\Lambda$.

Finally, to further confirm our analytical strong coupling theory, we compare in Fig. 9 the MSD simulated by the full model of Eq. (7) with the analytical expression (40). To obtain the ensemble average for the simulated MSD, we disregarded the initial parts of the trajectories which had not reached the stochastic limit cycle. Both curves in Fig. 9 show the high-frequency oscillations of the MSD at small times and the diffusive limit at large times.

## IV. SUMMARY

Our model describes the dynamics of self-propelled microorganisms that show chemotactic response to a chemical substrate, which is produced by the microorganisms themselves to attract or repel each other. Each particle moves with constant speed on a surface while its velocity direction diffuses and tends to align along the concentration gradient of the chemical.

Here we concentrated on the analysis of a single autochemotactic walker, which reacts to its own secreted chemical. We analyzed how the chemotactic coupling determines the long-time diffusive dynamics. Our main goal was to derive analytical expressions for the diffusion coefficient and to confirm their validity by simulations. In particular, we showed that adjusting the effective chemotaxis strength $\Lambda$ enables to alter the diffusion coefficient by several orders of magnitude. In nature, a variation in $\Lambda$ might arise from environmental influences that change the production rate of the chemical or directly the chemotactic coupling $\kappa$. Since we can adjust the speed $v$ and diffusion coefficient $D_{\rm eff}$ independently, we expect our model to be applicable to a large variety of microorganisms.

Whereas for weak chemotactic coupling, the walker's velocity direction diffuses with a modified noise strength (Sec. III A), the dynamics for strong coupling corresponds to rotational diffusion with an additional angular drift velocity (Sec. III B). However, a rigorous calculation of the effective noise in the second case could not be achieved.

For attractive autochemotaxis, our model describes the formation of particle clusters and thus represents a communication mechanism between microorganisms, as it is, for instance, required for bacterial colonization or biofilm formation. To make the model more realistic, we plan to incorporate repulsive interactions between individual walkers and to study the dynamics of particle collisions and cluster formation [55].

## ACKNOWLEDGMENTS

We thank Carsten Beta and Matthias Theves for helpful discussions. This work was funded by the Research Training Group GRK 1558 "Nonequilibrium Collective Dynamics in Condensed Matter and Biological Systems" of the Deutsche Forschungsgemeinschaft and DFG Grant No. ZA593/2-1 (VZ).

## APPENDIX A: DERIVATION OF THE LANGEVIN EQUATION FOR WEAK CHEMOTACTIC COUPLING

In the case of weak chemotactic coupling treated in Sec. III A, the particle motion is effectively described by the Langevin equation (24) for rotational diffusion with modified noise strength. Here we present details of the derivation.

Using $\zeta = v^2/(4D_c) + k$ the exponential in the expression of the chemical's gradient (21) is written as $\exp[-\zeta ut + \mathcal{O}(u^3)]$. Up to second order in $u$, Eq. (21) therefore becomes

$$\nabla c(\mathbf{r}_a(t),t) = \left(-\frac{h}{8\pi D_c^2}\int_{\tau_{\rm del}/t}^1 {\rm d}u\ \frac{e^{-\zeta ut}}{u}\right)\dot{\mathbf{r}}_a(t) + \left(\frac{h}{16\pi D_c^2}\, t\int_{\tau_{\rm del}/t}^1 {\rm d}u\ e^{-\zeta ut}\right)\ddot{\mathbf{r}}_a(t), \quad \text{(A1)}$$

so the concentration gradient at position $\mathbf{r}_a(t)$ is proportional to the velocity $\dot{\mathbf{r}}_a(t)$ and the acceleration $\ddot{\mathbf{r}}_a(t)$ of the particle. To proceed, we only need to take into account the integral in the second term. Due to $kt \gg 1$ we also have $\zeta t \gg 1$ and thus approximate $t\int_{\tau_{\rm del}/t}^1 {\rm d}u\ \exp(-\zeta ut) \approx \exp(-\zeta\tau_{\rm del})/\zeta$. Altogether we have

$$\nabla c(\mathbf{r}_a(t),t) = [\cdots]\, v\,\mathbf{e}(t) + \frac{h}{16\pi D_c^2}\,\frac{e^{-\zeta\tau_{\rm del}}}{\zeta}\, v\,\dot{\mathbf{e}}(t). \quad \text{(A2)}$$

Now we insert the chemotactic force $\mathbf{E}(\mathbf{r}_a(t),t) = \kappa\nabla c(\mathbf{r}_a(t),t)$ into Eq. (5) for the unit vector:

$$\frac{{\rm d}\mathbf{e}}{{\rm d}t} = \frac{1}{\gamma_{\rm R}}(\mathbb{1} - \mathbf{e}\otimes\mathbf{e})\left[[\cdots]\,\mathbf{e}(t) + \kappa\,\frac{hve^{-\zeta\tau_{\rm del}}}{16\pi D_c^2\zeta}\,\dot{\mathbf{e}}(t)\right] + \text{"noise term."} \quad \text{(A3)}$$

Using the fact that $(\mathbb{1} - \mathbf{e}\otimes\mathbf{e})$ is a projection operator onto the space perpendicular to $\mathbf{e}$ and the property $\mathbf{e}\perp\dot{\mathbf{e}}$ only the second summand in Eq. (A3) contributes. As it is proportional to $\dot{\mathbf{e}}(t)$ we can write the equation of motion as

$$\left(1 - \frac{\kappa}{\gamma_{\rm R}}\,\frac{hve^{-\zeta\tau_{\rm del}}}{16\pi D_c^2\zeta}\right)\frac{\rm d}{{\rm d}t}\,\mathbf{e}(t) = \text{"noise term."} \quad \text{(A4)}$$

By rewriting Eq. (A4) in terms of the angle we obtain the Langevin equation given by expression (24).

## APPENDIX B: CALCULATION OF THE MSD FOR ROTATIONAL DIFFUSION WITH CONSTANT ANGULAR DRIFT

The aim of the subsequent calculation is to work out an expression for the MSD $\langle[\mathbf{r}_a(t) - \mathbf{r}_a(0)]^2\rangle$ of a particle whose velocity direction satisfies Langevin equation (39) for rotational diffusion with constant drift. Let us first compute the correlation function for the velocity direction $\langle\mathbf{e}(t)\cdot\mathbf{e}(0)\rangle = \langle\cos[\varphi(t) - \varphi(0)]\rangle$. The formal solution of Eq. (39) with initial condition $\varphi(t=0) = \varphi(0)$ is given by $\varphi(t) = \varphi(0) + \omega t + \sqrt{2q}\int_0^t {\rm d}t'\ \Gamma(t')$. It follows that

$$\langle\mathbf{e}(t)\cdot\mathbf{e}(0)\rangle = \cos(\omega t)\left\langle\cos\left[\sqrt{2q}\int_0^t {\rm d}t'\ \Gamma(t')\right]\right\rangle - \sin(\omega t)\left\langle\sin\left[\sqrt{2q}\int_0^t {\rm d}t'\ \Gamma(t')\right]\right\rangle. \quad \text{(B1)}$$

For noise $\Gamma(t)$ that is a stationary process with Gaussian distribution and zero mean value, the following relationship

holds [29]:

$$\left\langle \exp\left[a\int_0^t \mathrm{d}t'\,\Gamma(t')\right]\right\rangle = \exp\left[\frac{a^2}{2}\int_0^t \mathrm{d}t'\int_0^t \mathrm{d}t''\,\langle\Gamma(t')\Gamma(t'')\rangle\right]. \quad \text{(B2)}$$

Since $\langle\Gamma(t')\Gamma(t'')\rangle = \delta(t'-t'')$, we can perform the double integral and obtain by setting $a = i\sqrt{2q}$,

$$\left\langle \exp\left[i\sqrt{2q}\int_0^t \mathrm{d}t'\,\Gamma(t')\right]\right\rangle = \exp(-qt). \quad \text{(B3)}$$

The imaginary part of (B3) is zero, so that Eq. (B1) becomes $\langle \mathbf{e}(t)\cdot\mathbf{e}(0)\rangle = \cos(\omega t)\,e^{-qt}$. Rewritten for arbitrary times $t, t'$, one has

$$\langle \mathbf{e}(t)\cdot\mathbf{e}(t')\rangle = \cos(\omega|t-t'|)\,e^{-q|t-t'|}. \quad \text{(B4)}$$

Integrating the velocity direction vector provides the particle position $\mathbf{r}_a(t) = \mathbf{r}_a(0) + v\int_0^t \mathrm{d}t'\,\mathbf{e}(t')$ and the MSD is then calculated as

$$\langle[\mathbf{r}_a(t)-\mathbf{r}_a(0)]^2\rangle = v^2\int_0^t \mathrm{d}t'\int_0^t \mathrm{d}t''\,\langle\mathbf{e}(t')\cdot\mathbf{e}(t'')\rangle. \quad \text{(B5)}$$

Performing the double integral in (B5) gives the final result from Eq. (40).


[1] E. Ben-Jacob, I. Cohen, and H. Levine, Adv. Phys. **49**, 395 (2000).
[2] D. Bray, *Cell Movements: From Molecules to Motility*, 2nd ed. (Garland Publishing, New York, 2001).
[3] J. D. Murray, *Mathematical Biology I. An Introduction*, 3rd ed., Vol. 1 (Springer, New York, 2001).
[4] M. Eisenbach, *Chemotaxis* (Imperial College Press, London, 2004).
[5] J. S. King and R. H. Insall, Trends Cell Biol. **19**, 523 (2009).
[6] N. Mittal, E. O. Budrene, M. P. Brenner, and A. van Oudenaarden, Proc. Natl. Acad. Sci. USA **100**, 13259 (2003).
[7] L. Hall-Stoodley, J. W. Costerton, and P. Stoodley, Nat. Rev. Microbiol. **2**, 95 (2002).
[8] Q. Wang and T. Zhang, Solid State Commun. **150**, 1009 (2010).
[9] R. M. Donlan and J. W. Costerton, Clin. Microbiol. Rev. **15**, 167 (2002).
[10] E. F. Keller and L. A. Segel, J. Theor. Biol. **26**, 399 (1970); *ibid.* **30**, 225 (1971).
[11] T. Hillen and K. Painter, J. Math. Biol. **58**, 183 (2009).
[12] M. J. Tindall, S. L. Porter, P. K. Maini, G. Gaglia, and J. P. Armitage, Bull. Math. Biol. **70**, 1525 (2008).
[13] M. J. Tindall, P. K. Maini, S. L. Porter, and J. P. Armitage, Bull. Math. Biol. **70**, 1570 (2008).
[14] T. Hillen and H. G. Othmer, SIAM J. Appl. Math. **61**, 751 (2000); H. G. Othmer and T. Hillen, *ibid.* **62**, 1222 (2002).
[15] T. J. Newman and R. Grima, Phys. Rev. E **70**, 051916 (2004).
[16] A. Sengupta, S. van Teeffelen, and H. Löwen, Phys. Rev. E **80**, 031122 (2009).
[17] H. Löwen and G. Szamel, J. Phys. Condens. Matter **5**, 2295 (1993).
[18] D. S. Dean and A. Lefèvre, Phys. Rev. E **69**, 061111 (2004).
[19] R. Grima, Phys. Rev. Lett. **95**, 128103 (2005).
[20] B. Lindner, New J. Phys. **9**, 136 (2007).
[21] B. Lindner, J. Stat. Phys. **130**, 523 (2007).
[22] P. H. Chavanis, Eur. Phys. J. B **57**, 391 (2007).
[23] C. Bracher, Physica A **331**, 448 (2004).
[24] Y. Tsori and P.-G. de Gennes, Europhys. Lett. **66**, 599 (2004).
[25] R. Grima, Phys. Rev. E **74**, 011125 (2006).
[26] T. A. M. Langlands and B. I. Henry, Phys. Rev. E **81**, 051102 (2010); S. Fedotov, *ibid.* **83**, 021110 (2011); F. Matthäus, M. Jagodic, and J. Dobnikar, Biophys. J. **97**, 946 (2009).
[27] D. B. Kearns, Nat. Rev. Microbiol. **8**, 634 (2010).
[28] E. A. Codling, M. J. Plank, and S. Benhamou, J. Roy. Soc. Interface **5**, 813 (2008).
[29] H. Risken, *The Fokker-Planck Equation*, 2nd ed. (Springer, New York, 1996).
[30] M. Schienbein and H. Gruler, Bull. Math. Biol. **55**, 585 (1993).
[31] F. Peruani and L. G. Morelli, Phys. Rev. Lett. **99**, 010602 (2007).
[32] L. H. Cisneros, J. O. Kessler, S. Ganguly, and R. E. Goldstein, Phys. Rev. E **83**, 061907 (2011).
[33] E. Sackmann, F. Keber, and D. Heinrich, Ann. Rev. Condens. Matter Phys. **1**, 257 (2010).
[34] J. P. Armitage, T. P. Pitta, M. A.-S. Vigeant, H. L. Packer, and R. M. Ford, J. Bacteriol. **181**, 4825 (1999).
[35] H. C. Berg, *E. coli in Motion* (Springer, New York, 2004).
[36] F. Schweitzer and L. Schimansky-Geier, Physica A **206**, 359 (1994).
[37] P. Romanczuk, U. Erdmann, H. Engel, and L. Schimansky-Geier, Eur. Phys. J. Special Topics **157**, 61 (2008).
[38] A. Sokolov, I. S. Aranson, J. O. Kessler, and R. E. Goldstein, Phys. Rev. Lett. **98**, 158102 (2007).
[39] Y. Xiong, C.-H. Huang, P. A. Iglesias, and P. N. Devreotes, Proc. Natl. Acad. Sci. USA **107**, 17079 (2010).
[40] A. Celani and M. Vergassola, Proc. Natl. Acad. Sci. USA **107**, 1391 (2010).
[41] T. Ahmed, T. S. Shimizu, and R. Stocker, Integr. Biol. **2**, 604 (2010).
[42] D. Fuller, W. Chen, M. Adler, A. Groisman, H. Levine, W.-J. Rappel, and W. F. Loomis, Proc. Natl. Acad. Sci. USA **107**, 9656 (2010).
[43] R. Thar and M. Kühl, Proc. Natl. Acad. Sci. USA **100**, 5748 (2003).
[44] P. A. Iglesias and P. N. Devreotes, Curr. Opin. Cell Biol. **20**, 35 (2008).
[45] M. Doi and S. F. Edwards, *The Theory of Polymer Dynamics*, Vol. 73 (Clarendon Press, Oxford, 2001).
[46] E. Lauga and T. R. Powers, Rep. Prog. Phys. **72**, 096601 (2009).
[47] W. T. Coffey, Y. P. Kalmykov, and J. T. Waldron, *The Langevin Equation: With Applications to Stochastic Problems in Physics, Chemistry and Electrical Engineering* (World Scientific, Singapore, 1998).
[48] W. Horsthemke and R. Lefever, *Noise-Induced Transitions* (Springer, New York, 1984).

[49] P. E. Kloeden and E. Platen, *Numerical Solution of Stochastic Differential Equations* (Springer, New York, 1992).
[50] H. Goldstein, C. P. Poole, and J. L. Safko, *Classical Mechanics*, 3rd ed. (Addison Wesley, Nw York, 2001).
[51] H. Gruler and K. Franke, Z. Naturforsch. C **45**, 1241 (1990).
[52] M. Schienbein, K. Franke, and H. Gruler, Phys. Rev. E **49**, 5462 (1994).
[53] A. Czirók, E. Ben-Jacob, I. Cohen, and T. Vicsek, Phys. Rev. E **54**, 1791 (1996).
[54] P.-H. Chavanis, Comm. Nonlin. Sci. Numer. Simul. **15**, 60 (2010).
[55] J. Taktikos, V. Zaburdaev, and H. Stark (unpublished).
[56] H. Berg and E. Purcell, Biophys. J. **20**, 193 (1977).
[57] M. Luca, A. Chavez-Ross, L. Edelstein-Keshet, and A. Mogilner, Bull. Math. Biol. **65**, 693 (2003).
[58] H. C. Berg, *Random Walks in Biology* (Princeton University Press, Princeton, NJ, 1993).
[59] H. C. Berg and L. Turner, Biophys. J. **58**, 919 (1990).
[60] L. Li, S. F. Norelykke, and E. C. Cox, PLoS ONE **3**, e2093 (2008).
[61] R. G. Endres and N. S. Wingreen, Proc. Natl. Acad. Sci. USA **105**, 15749 (2008).
[62] J.-L. Martiel and A. Goldbeter, Biophys. J. **52**, 807 (1987).